

## **Using multiple downhole VSP arrays for monitoring passive microseisms**

Zuolin Chen and Robert R. Stewart

### **ABSTRACT**

Using a hypocenter location method, which depends on the P and S arrival times only, the hypocenter accuracy as determined by an observation network composed of one or more VSP arrays and several geophones in separate wells is calculated. Error analysis illustrates that the events recorded by this kind of seismic monitoring network can be located with an accuracy of 5m-10m within the network. Compared to the conventional VSP location methods which use hodograms and P and S arrival times, our method has the advantages of being convenient, reliable and much more accurate. Thus, we suggest using this kind of network to monitor passive microseismic activity and to locate the recorded events using P and/or S arrival times only in the future study. Besides, we also determined rules for the alignment of such networks.

### **INTRODUCTION**

Microseismic events are related to earth movements on pre-existing structures or new fractures. They may arise as the rock mass reacts to stresses and strains associated with pressure changes in a reservoir. Microseismicity can provide a wealth of information regarding fractures, reservoir scale production, injection-induced changes and rock properties.

The most fundamental information from passive seismic monitoring is the location of the microseismic events. The location procedure is generally accomplished by using single-well techniques. In principle, a 3-component geophone allows location of the event. The direction is derived from a hodogram analysis of the P-wave arrival and the distance from the P-S travel time difference. Using more than one geophone gives redundancy and thus better results. Besides using the P-S travel time difference, another classical method involves the inversion of P- and S-wave arrival times at different geophones (Fabriol, 2001; Chen and Stewart, 2006).

Needless to say, the hypocentral location uncertainty of the events is a key parameter for the seismic image quality. However, the accuracy using these conventional methods is generally no better than on the order of tens of meters and often requires many conditions to be met (Fabriol, 2001). Also, the determination of the back-azimuth or angle of inclination of an event from hodograms is often inaccurate and time consuming. Picking of the ambiguous S-phases is often problematic and can induce large error into the seismic images.

Hypocenter location using first-arrival times has long been used in earthquake research, and had been confirmed to be much better than using the back-azimuth and angle of inclination. Due to the special geometry of a downhole VSP array, location methods using arrival times alone are not generally used in monitoring the microseismicity in the oil reservoirs. In recent years, with the development of techniques

which need the installation of multiple downhole geophones, location of events using multiple or combinations of a VSP with single geophones in separate wells became possible. To examine the accuracy of location using arrival times, we tried to develop a fast and convenient error analysis computer program which can give the horizontal and vertical uncertainties of hypocenter locations on a 3-D spatial grid system. The algorithm for error analysis is based on the conventional error ellipsoid equation developed from the generalized normal equation (Flinn, 1965; Everdon, 1969). Using various multiple downhole VSP arrays or the combination of a VSP array with a single geophone in the nearby wells, the corresponding error distributions are derived and analyzed. In comparison with the mentioned location methods, we suggest that the multiple-well observation approach may be the most accurate and applicable one in future monitoring of the microseismicity in oil reservoirs.

## NUMERICAL EXPERIMENTS

The algorithm to calculate the error is described in detail in another CREWES Report (Chen, 2006). Generally, the one-standard error ellipsoids can be obtained from the equation developed by several workers (Flinn, 1965; Turcotte, 1967; Evernden, 1969). The results of maximum horizontal and vertical errors are illustrated at the nodes of a 3-D grid system. For convenience in visualization, errors are plotted as contour maps on a series of 2-D horizontal cross sections (depth cross sections).

### Pre-conditions of the numerical experiments

A constant velocity model (with P-wave velocity  $V_p=4000$  m/s) was chosen in this study. The advantages of a constant-velocity model lie in its simplicity, ease of interpretation and comparison of results from various array configurations. The model of the VSP downhole array is based on the real VSP array deployed by Lawton et al. (2005) in Violet Grove, central Alberta, where the eight 3-C geophones are installed from 1400m to 1540m beneath the surface at an interval of 20m.

The picking error, as the prior data variance, is assumed to be known beforehand, and the P-arrivals (that is  $\sigma_i$ ,  $i=1$  to  $N$ ) is assumed to be a function of the epicentral distance of an event to the receiver ( $D_i^{epi}$ ). It increases with  $D_i^{epi}$  as a step function as follows:

$$\begin{aligned} \sigma_i &= 0.001 \text{ sec} && (D_i^{epi} \leq D_{max}^{array}/2); \\ \sigma_i &= 0.002 \text{ sec} && (D_{max}^{array}/2 < D_i^{epi} \leq D_{max}^{array}); \\ \sigma_i &= 0.004 \text{ sec} && (D_i^{epi} > D_{max}^{array}); \end{aligned}$$

where  $D_{max}^{array}$  is the maximum lateral interval between receivers of the VSP and newly-added geophones in the nearby wells. This variable standard picking error also functions as a kind of weighting factor, which enhances the effects of nearby stations and reduces the effect of distant ones.

Every event is recorded by all stations though that assumption is not required in real hypocenter location procedures.

In the numerical experiments, since the assumed velocity model to create the synthetic travel data of events and the model used for relocation of the events are the same, systematic error caused by the velocity model is removed. Thus the picking error will be the only source of input error.

To produce the error contour maps and plot error ellipses, events are aligned on a grid with a spacing of 50m in both easting and northing. Errors in both the horizontal and depth direction are viewed by introducing a series of horizontal parallel cross sections with a spacing interval of 20m in depth. To simplify the question, events on the nodes of the grid are assumed to be relocated back to their original positions.

### Case 1: VSP and two other geophone receivers

The error distribution in the case of the monitoring network composed of a VSP array and two other newly-added geophone receivers at the top level of VSP array is calculated. The 3-D positions of the geophones in the network is shown in Fig. 1a, where the depths of the two newly-added geophones are assumed to be at the same level as the top geophone of the existing VSP, with a lateral spacing of 400m in easting and northing respectively.

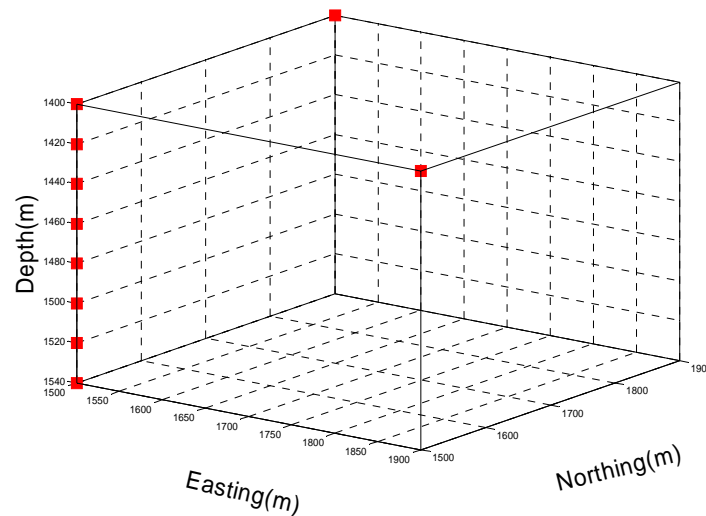


FIG. 1a. Geometry of the VSP and the two newly-added geophones at the top level of VSP array in two other separate wells.

Figures 1b and 1c illustrate the maximum horizontal and vertical distributions of the one-standard-error (68%) distribution on the horizontal cross sections from a depth of 1380m to 1540m. For convenience, we will omit the word “maximum” in front of the term “maximum horizontal and vertical errors” from now on.

The major features of the distributions of the horizontal errors are: errors are only 5m-20m in most areas within the frame of the network; in the vicinity of the VSP, errors are generally as small as 5m-10m. There is little change of the pattern within the range of studied depths. Outside the frame, errors increase rapidly with the epicentral distance to the nearby geophone or geophone array. It should be noted that in the shallowest slice at

1380m, which is 20m above the top geophone of the VSP array, horizontal errors are very unstable right above the VSP array. This indicates that the horizontal errors above the range of the VSP array could be very large.

Similar to the horizontal errors, vertical errors can also be located in a quite good accuracy of 5m-30m in most areas within the frame of the network throughout the study depth. In the vicinity of the VSP array, errors can be constrained to only 5m or less. This accuracy is considerably higher and much better than the results derived from the traditional location methods (we will compare the errors in the discussion section). Outside the frame of the array, errors increase from approximately 30m to 100m in the study area.

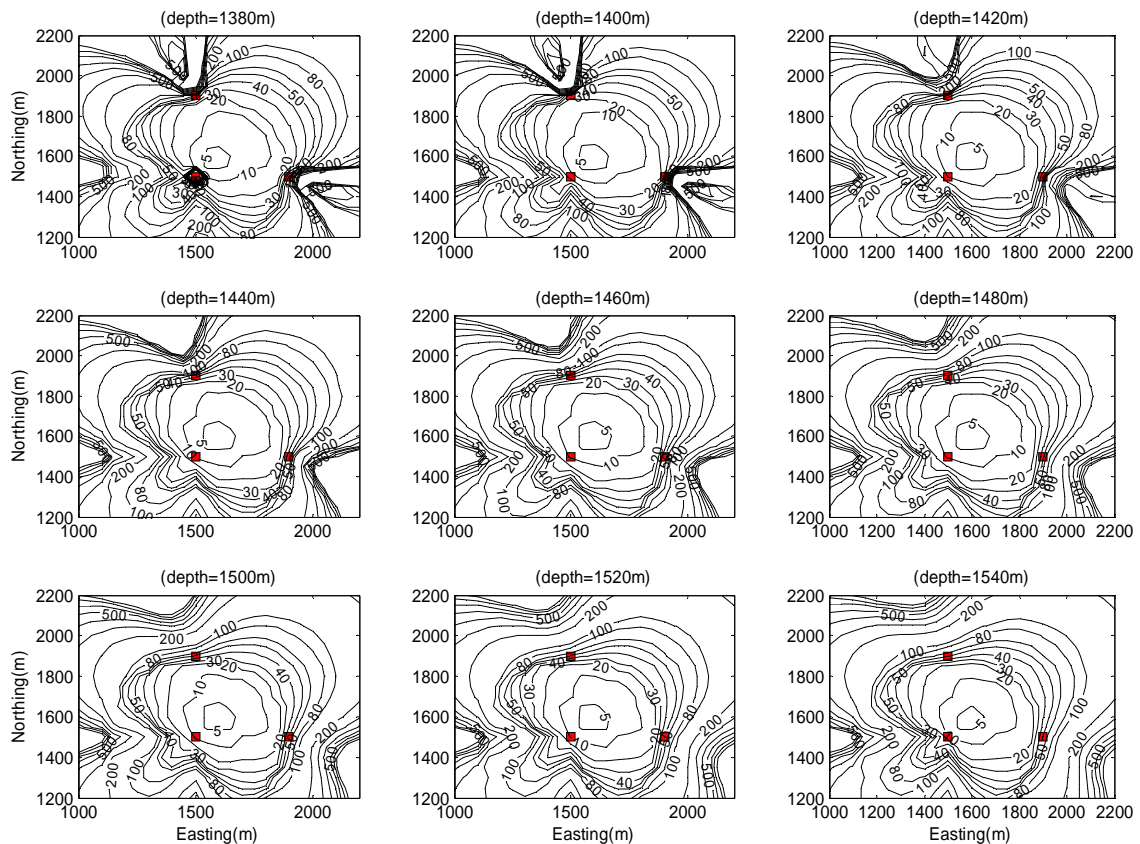


FIG. 1b. Horizontal cross sections of the one-standard horizontal errors (northing-easting) located by using an network composed of a VSP and two newly-added geophones at the top level of the VSP array in other two separate wells. The stations are denoted by red solid squares.

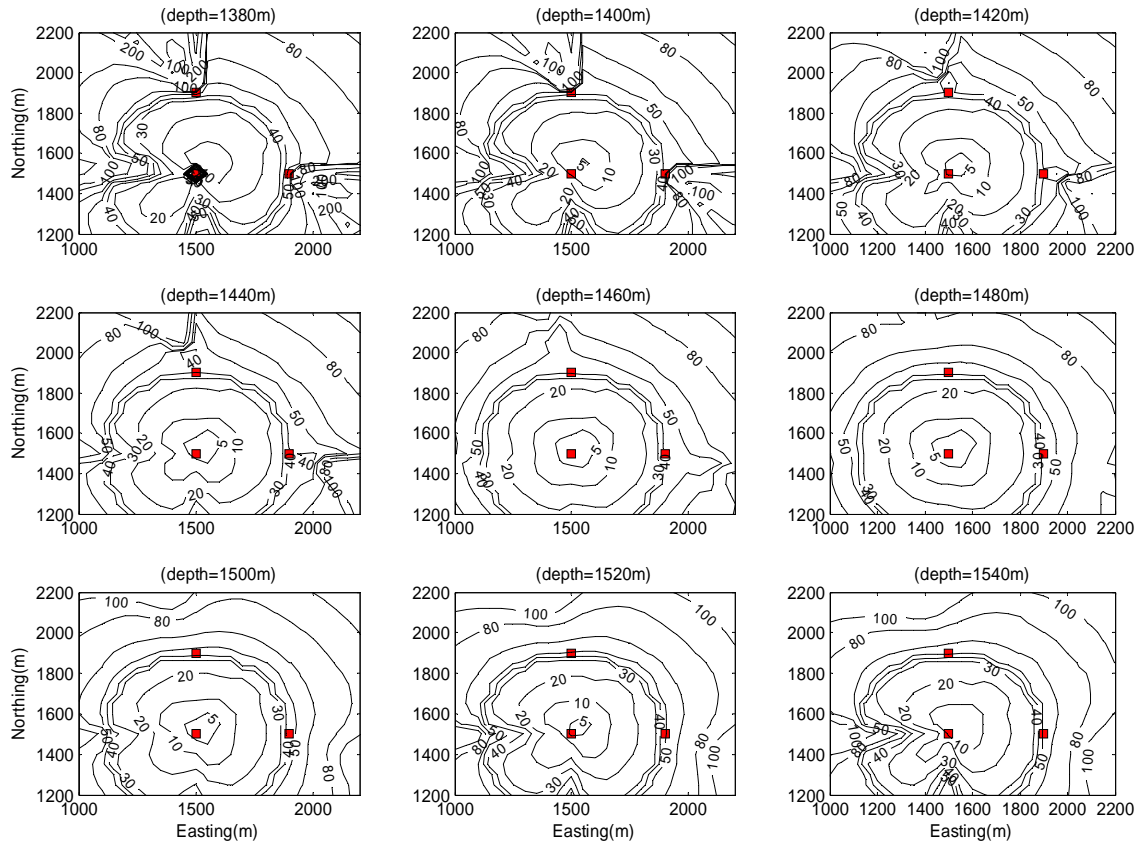


FIG. 1c. Horizontal cross sections of the one-standard vertical errors (northing-easting) located by using a network composed of a VSP and two newly-added geophones at the top level of the VSP array in other two separate wells. The stations are denoted by red solid squares.

### Case 2: VSP and geophone receivers at a medium depth

The error distribution in the case of the network composed of a VSP and two other newly-added geophones at a medium depth is calculated. The 3-D positions of the network is shown in Figure 2a, where the depth of the two newly-added geophones is assumed to be at the same level at the middle depth of the VSP(1470m), with a lateral spacing of 400m in easting and northing respectively.

Figure 2b and 2c illustrate the horizontal and vertical distributions of the one-standard-error on the horizontal cross sections from a depth of 1380m to 1540m separately. The major features of the distributions of the horizontal and vertical errors are very similar to the preceding Case 1 both in patterns and values except for some slight variations. This indicates that the effect of the depths of the newly-added geophones on the error distribution is insignificant when they are deployed within the depth range of the VSP array.

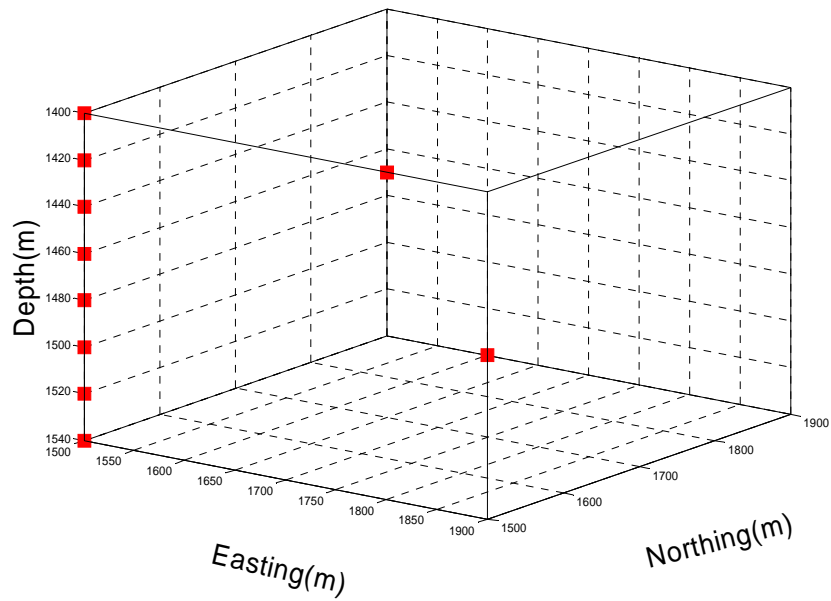


FIG. 2a. Geometry of the VSP and the two newly-added geophones at a medium depth in two separate wells.

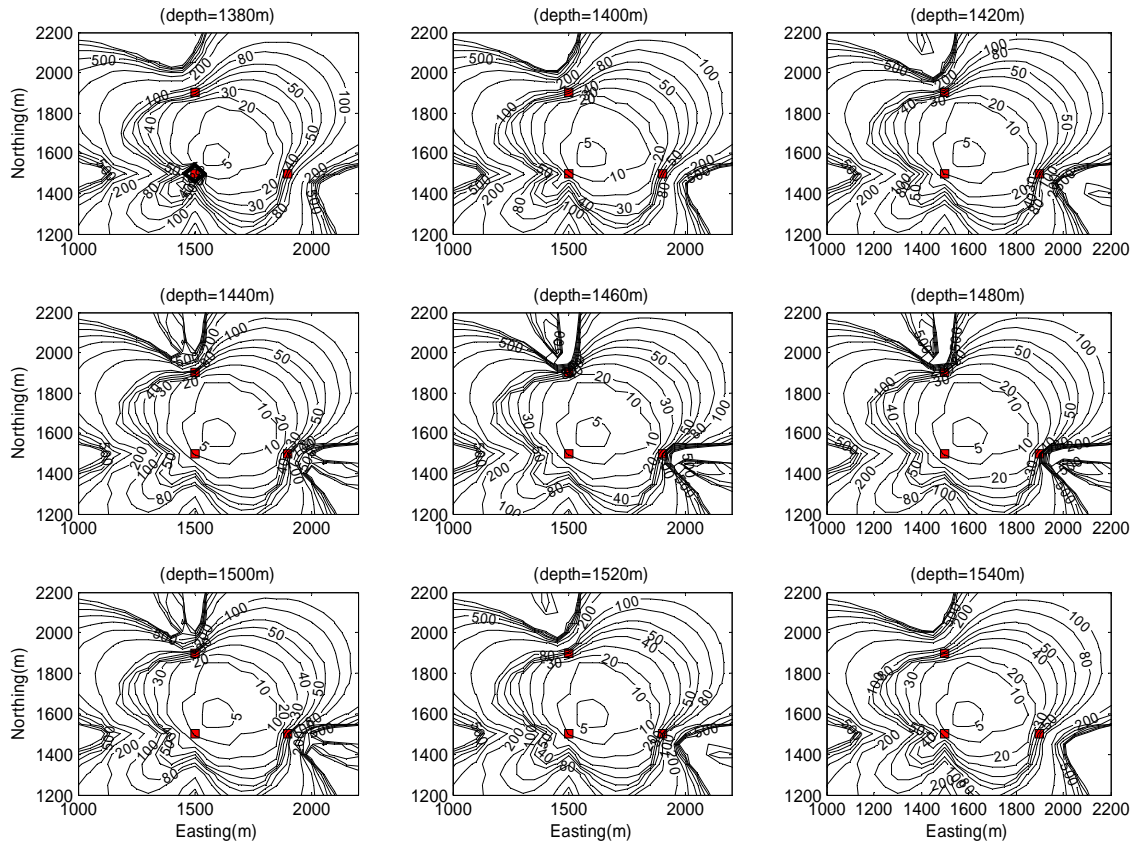


FIG. 2b. Horizontal cross sections of the one-standard horizontal errors determined by using a network composed of a VSP array and two newly-added geophones at a medium depth. The stations are denoted by red solid squares.

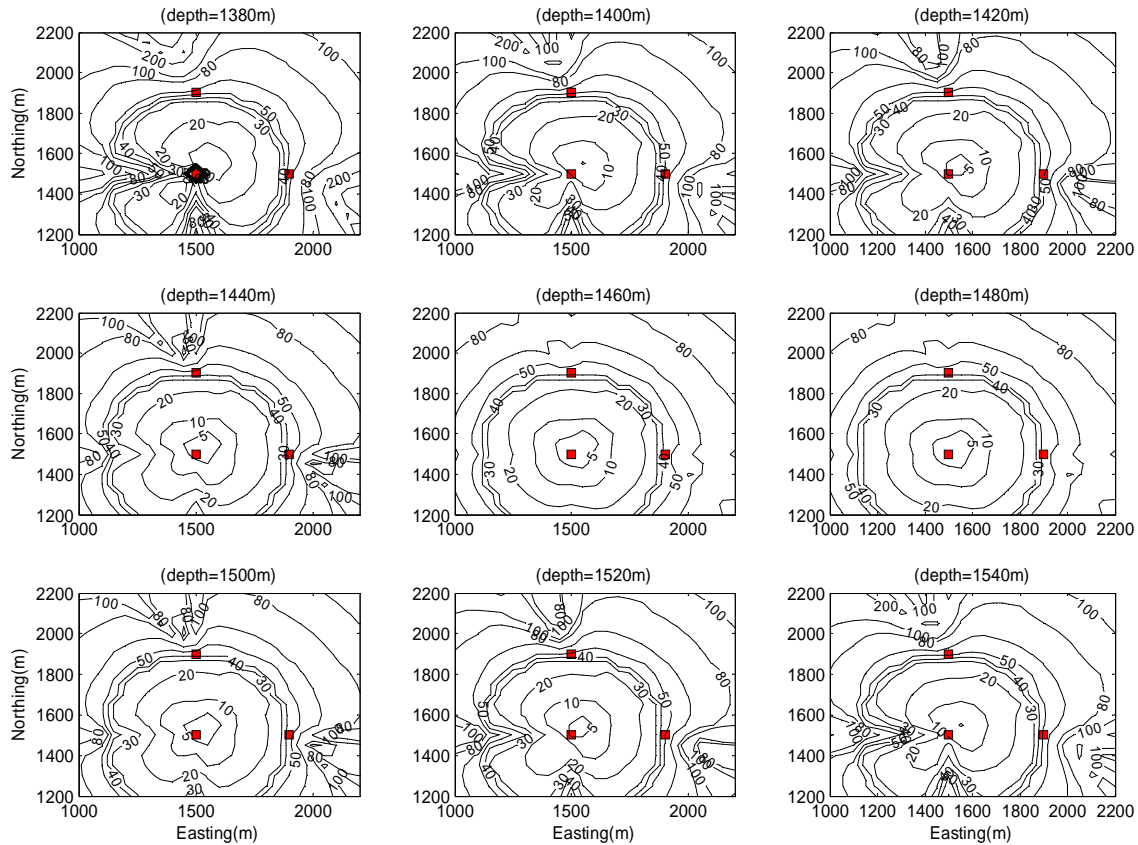


FIG. 2c. Horizontal cross sections of the one-standard vertical errors (northing-easting) determined by using a network composed of a VSP and two newly-added geophones at a medium depth. The stations are denoted by red solid squares.

### Case 3: VSP and two geophones at small distances

We have confirmed that the effect of the depth of the newly-added geophones to the errors is insignificant when they are deployed within the depth range of the VSP array. From this experiment on, the newly-added geophones are generally assumed to be deployed at a medium depth of 1470m except in the cases of using newly-added VSP array(s).

In practice, the distances between oil wells may vary from case to case. To confirm the effect of the scale of the network, a network at a smaller scale is considered. In this case, the distances between the two newly-added geophones assumed to be 150m and 200m away from the VSP array in northing and easting. The error distributions in the case are illustrated in Figures 3a and 3b.

Compared with results of the preceding cases, the patterns of the errors are similar within the frame of the network, but the constraint on the errors outside the network is much weaker. Inside the network, horizontal errors are located to 10m in most areas, which is slightly larger than the results in Case 1 and Case 2. On the other hand, vertical errors are almost unaffected.

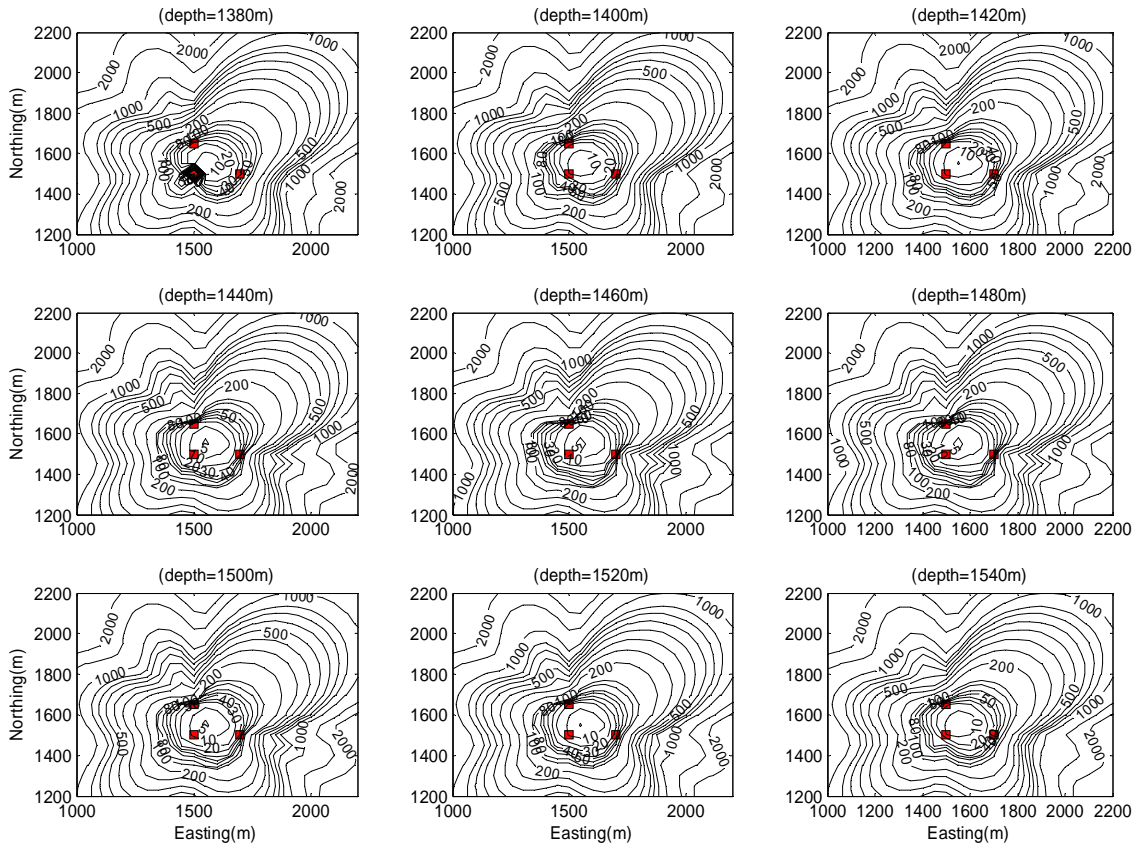


FIG. 3a. Horizontal cross sections of the one-standard horizontal errors determined by using a smaller network composed of a VSP array and two newly-added geophones at a medium depth. The stations are denoted by red solid squares.

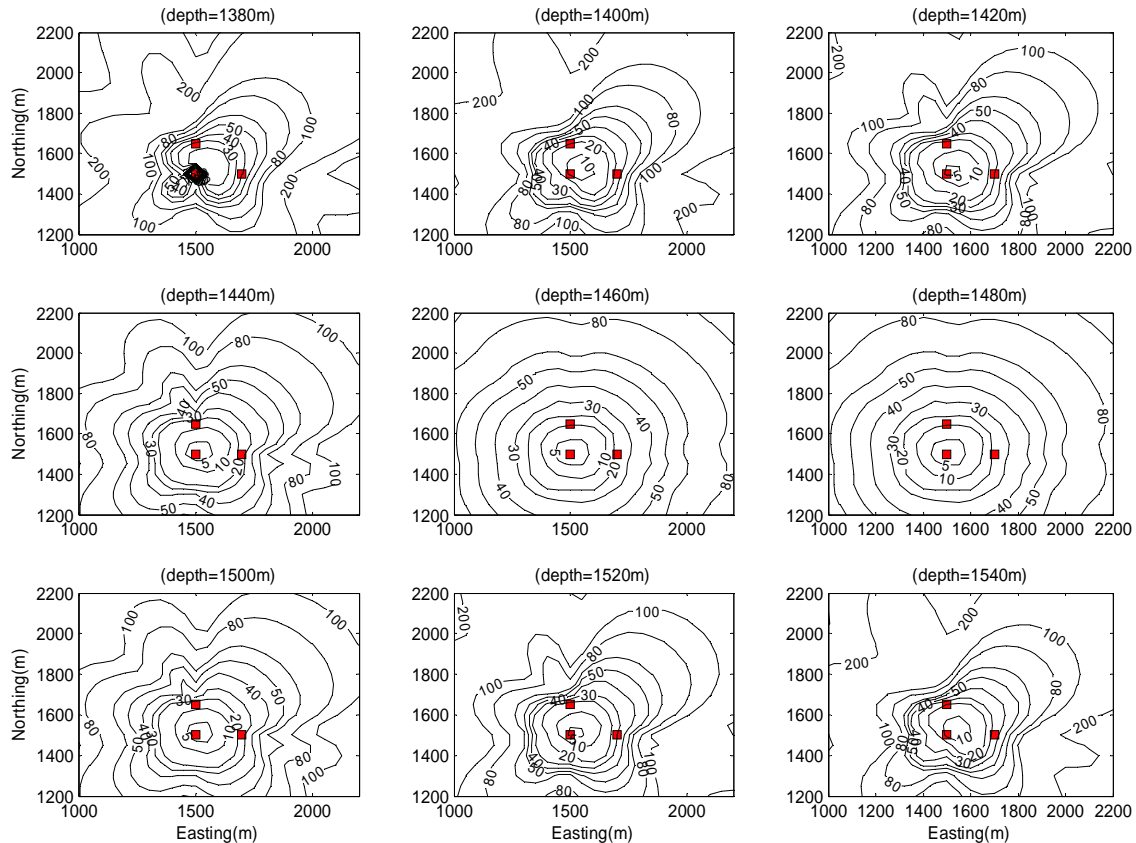


FIG. 3b. Horizontal cross sections of the one-standard vertical errors determined by using a smaller network composed of a VSP array and two newly-added geophones at a medium depth. The stations are denoted by red solid squares.

#### Case 4: Two VSP arrays and one geophone receiver

Suppose a case of a network formed by two VSP arrays and one geophone. In this case, the newly-added VSP array consisting of 8 geophones in the same depths as the previous VSP array, and the distance between them is 400m. The single geophone is arranged 400m in the northing (Figure 4a).

Figures 4b and 4c illustrate the horizontal and vertical distributions of the one-standard-errors on the horizontal cross sections from a depth of 1380 m to 1540 m separately. Different with the results of Case 1 and Case 2, the horizontal errors are further reduced to 5-10m within the frame and even in some areas outside the array in almost every horizontal cross section. Errors tend to be smaller when an event occurs close to the two VSP arrays, especially to the pre-existing one half-surrounded by the newly-added VSP array and the single geophone. For the vertical errors, the 10m-contour expands in all directions of the two VSP arrays, and the events between them can be located with an accuracy of 5m-10m.

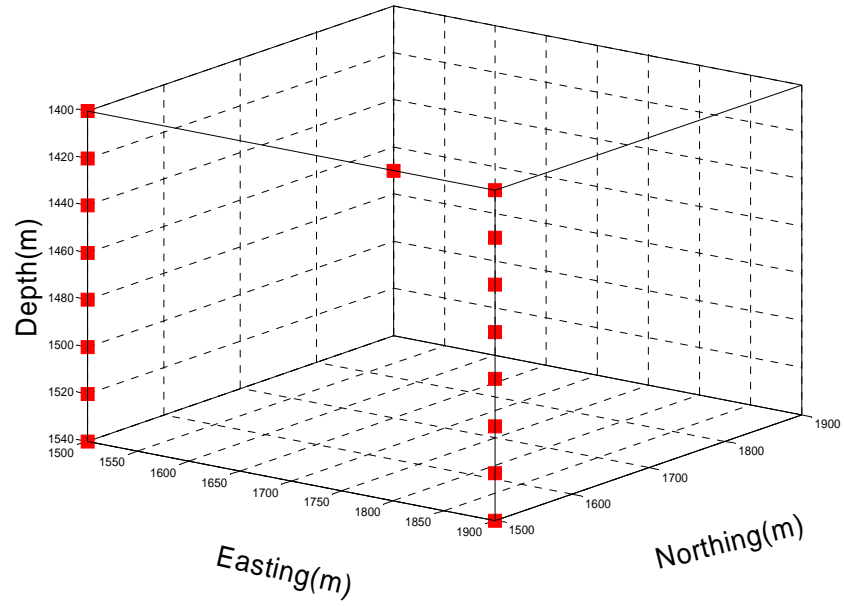


FIG. 4a. Geometry of the two VSP arrays and one geophone at a medium depth in another well.

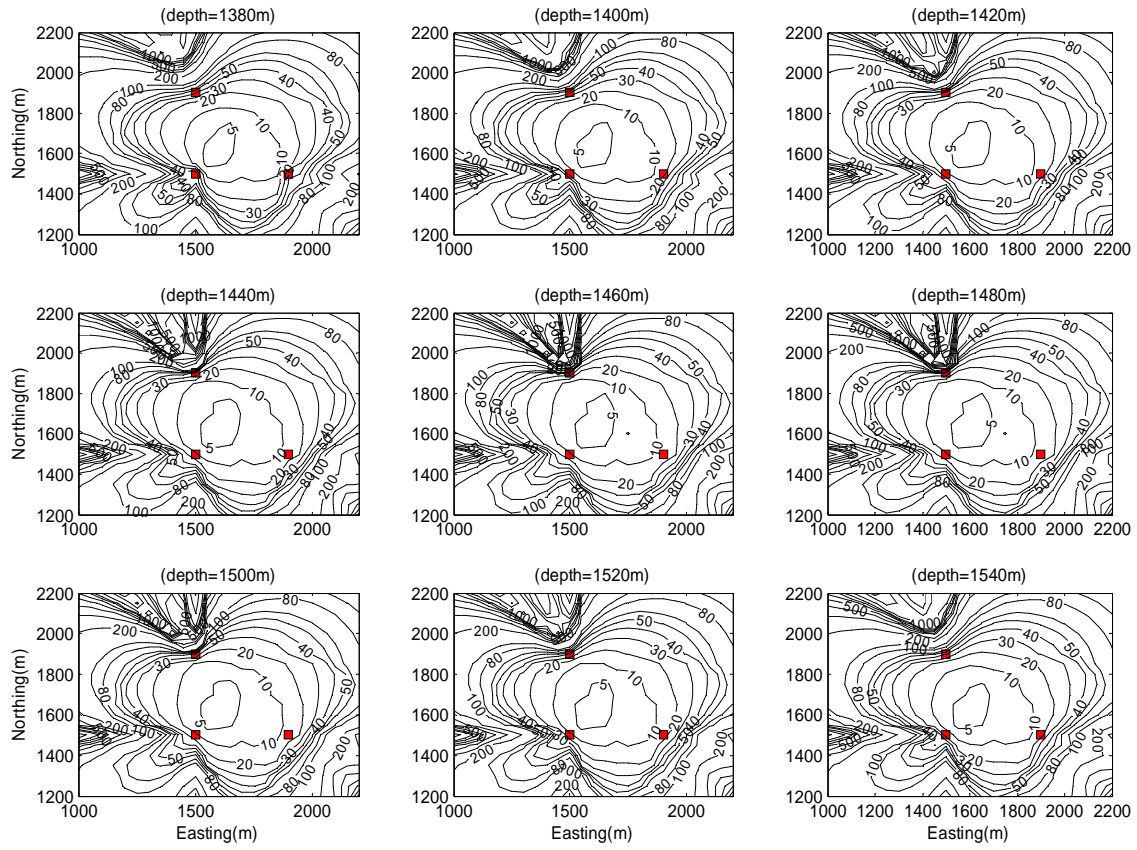


FIG. 4b. Horizontal cross sections of the one-standard horizontal errors (northing-easting) located by using a smaller network composed of two VSP arrays and one newly-added geophone at a medium depth. The stations are denoted by red solid squares.

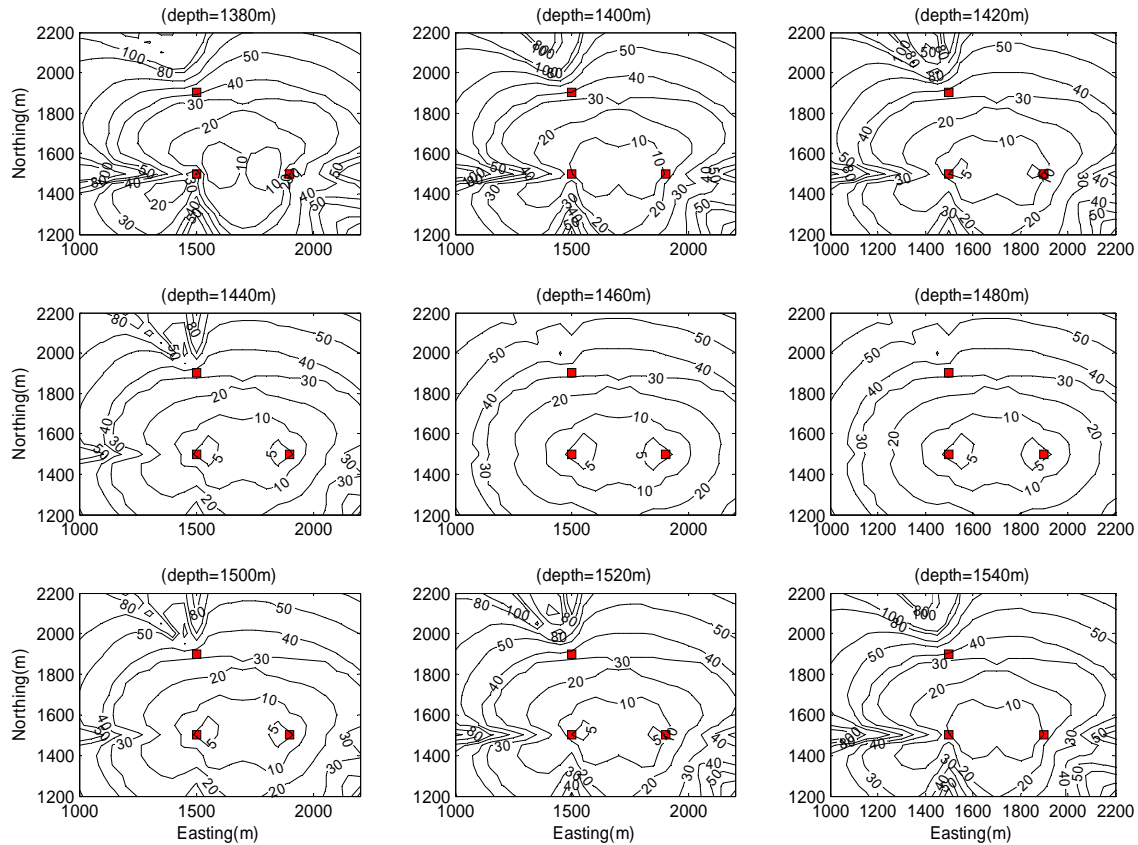


FIG. 4c. Horizontal cross sections of the one-standard vertical errors (northing-easting) located by using a smaller network composed of two VSP arrays and one newly-added geophone at a medium depth. The stations are denoted by red solid squares.

### Case 5: Three VSPs

In some ideal situations, multiple VSP arrays may be deployed in a small area. In this case, events can be located by a network composed of three or more VSP arrays. We assumed the case of three-VSP network, where all the VSP arrays consist of 8 geophones in the same depth distributions separately (Figure 5a). The distances between the existing VSP array and the two newly-added ones are both 400m east and north respectively.

Figures 5b and 5c show the horizontal and vertical distributions of the one-standard-errors on the horizontal cross sections from a depth of 1380m to 1540m. Different from the results of two-VSP Case 4, the horizontal errors are almost located less than 5m within the whole frame in all horizontal cross sections. Vertical errors throughout the study area and depth are less than 10m.

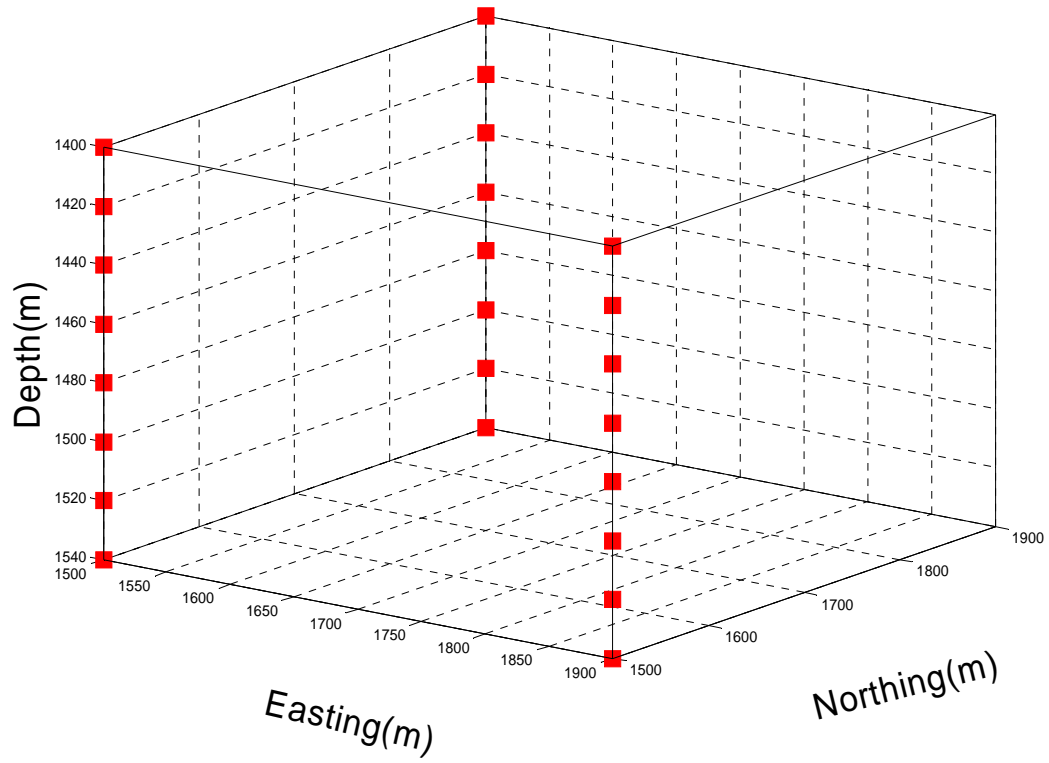


FIG. 5a. Geometry of the three VSP arrays.

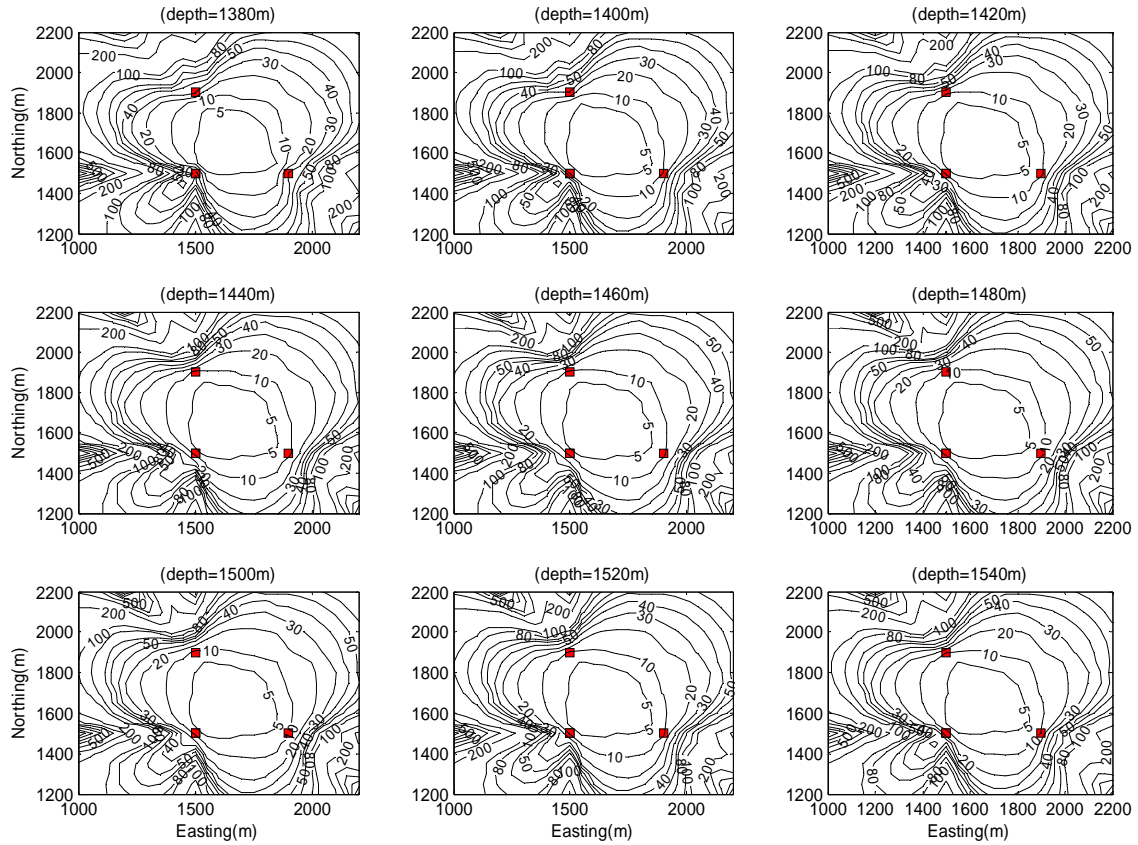


FIG. 5b. Horizontal cross sections of the one-standard horizontal errors determined by using a smaller network composed of three VSP arrays. The stations are denoted by red solid squares.

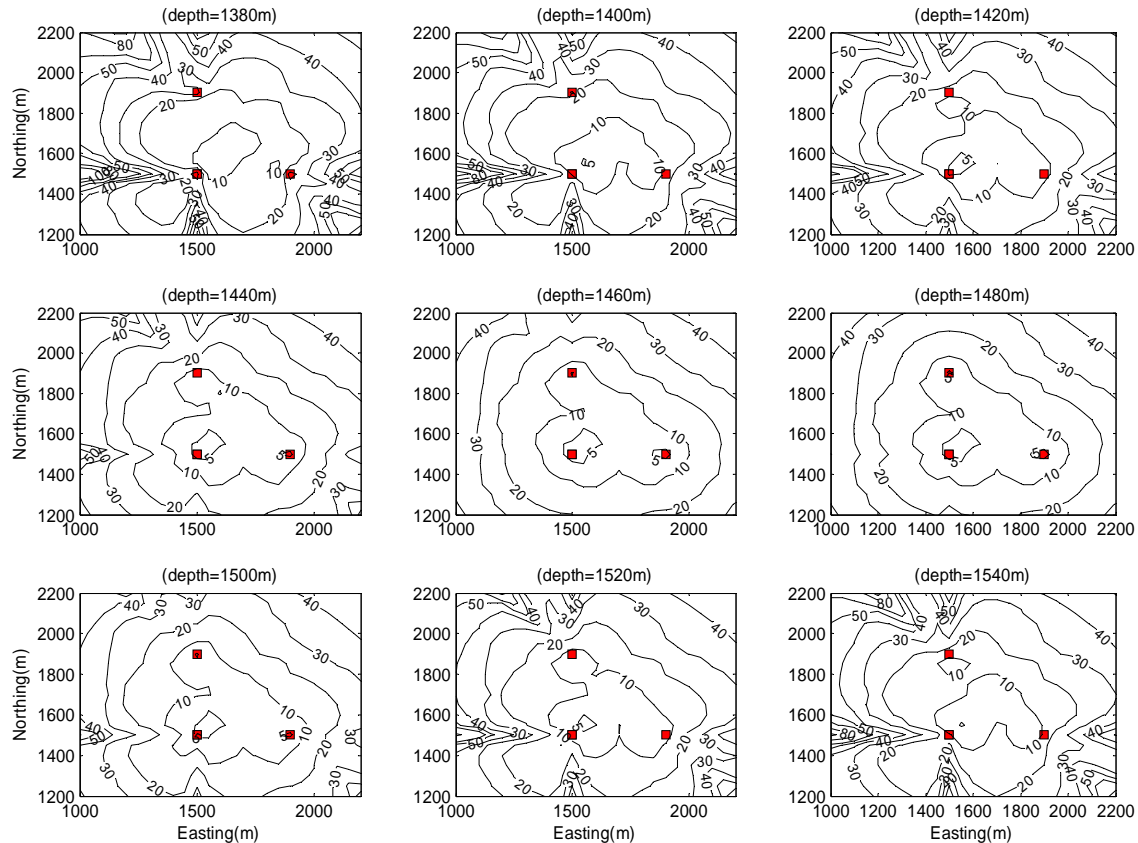


FIG. 5c. Horizontal cross sections of the one-standard vertical errors (northing-easting) located by using a smaller network composed of three VSP arrays. The stations are denoted by red solid squares.

### Case 6: VSP array and multiple geophone receivers

Although the 3-VSP network seems ideal for the location of the events within the frame, the accuracy of location can be improved a great deal as well in the case that an existing VSP array is surrounded by geophones installed in multiple wells. Consider a simplified case where three geophones are installed in three surrounding wells separately (Figures 6a and 6b).

From the results of the error distributions, horizontal errors are determined to be less than 5m in the vicinity of the VSP array. The radius of the 5m-contour surrounding the VSP array is approximately half the distance between the VSP array and any of the geophones. This means that this combination of geophones is quite applicable in real observations for the monitoring of the seismicity near the VSP array. In the same way, vertical errors in the vicinity of the VSP array can also be located be less than 5m to 10m.

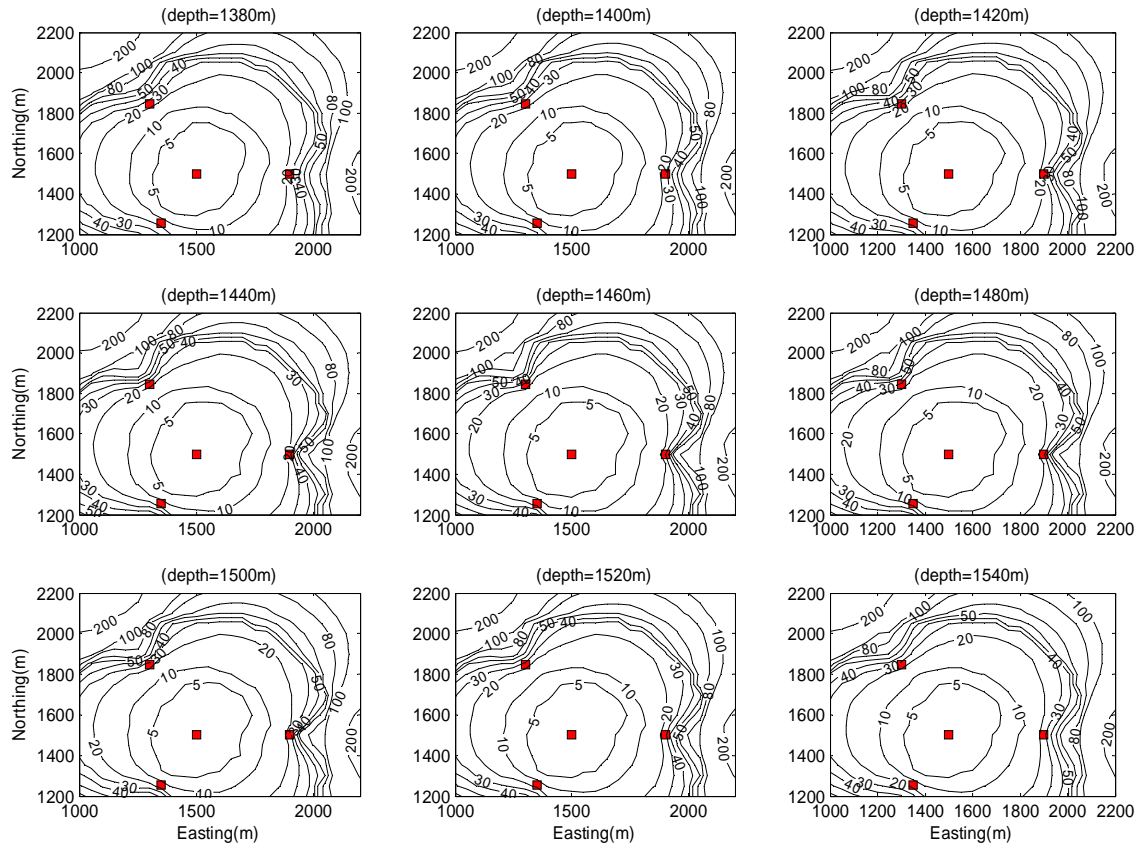


FIG. 6a. Horizontal cross sections of the one-standard horizontal errors determined by using a network composed of one VSP array and three surrounding geophones in three separate wells. The stations are denoted by red solid squares.

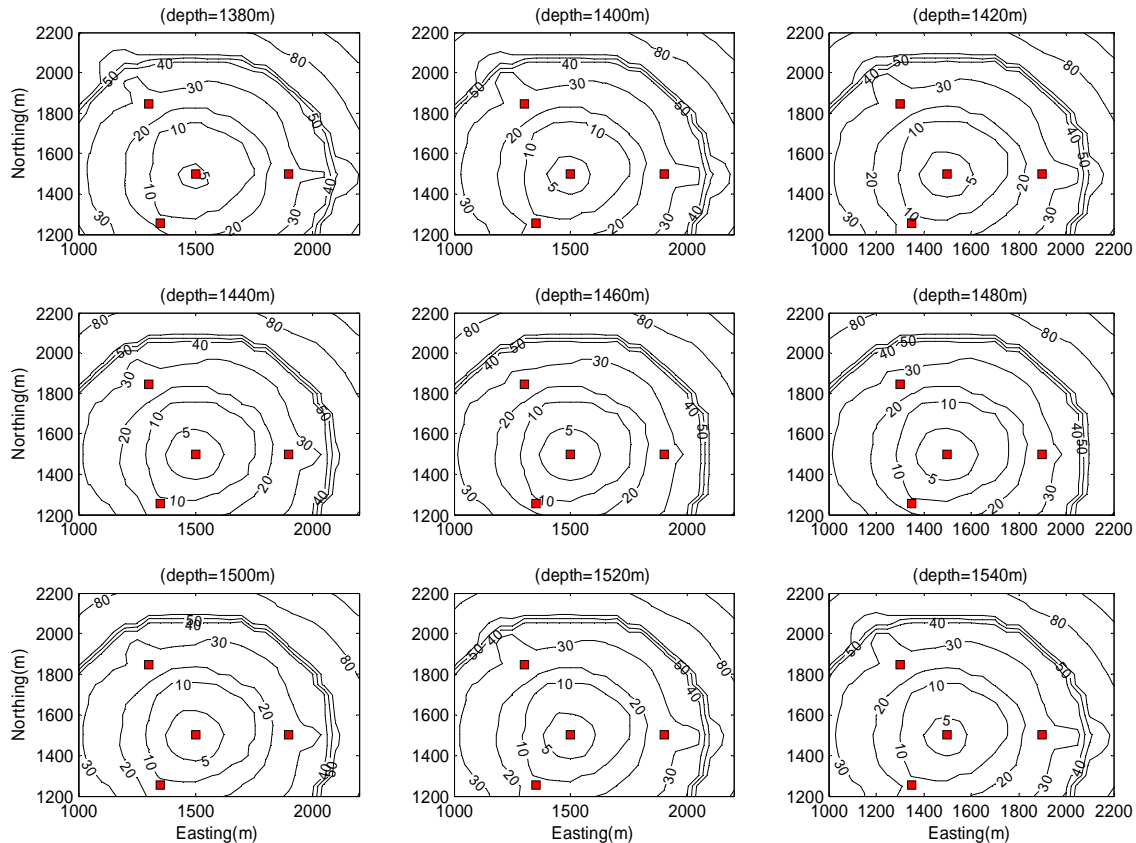


FIG. 6b. Horizontal cross sections of the one-standard vertical errors determined by using a network composed of one VSP array and three surrounding geophones in three separate wells. The stations are denoted by red solid squares.

## DISCUSSION

### Comparison of the errors determined by conventional location methods

The accuracy of the location of an event determined by using the back-azimuth and the angle of inclination from hodograms is generally on the order of tens of meters. To obtain this accuracy, some conditions like sampling frequency higher than 1000 KHz and accurate picking of arrival times must be met (Fabriol, 2001). The azimuth and inclination of propagation of the P-wave from the polarization of the first arrivals are often determined poorly (Phillips et al., 1998), and some times can not be used for the location. The lateral accuracy using the combination of back-azimuth and the inversion of P, S arrival times are estimated to be on the order of 20 m with the pre-condition of a small azimuth error of  $2.5^\circ$  within a radius of 400m from the VSP array; and the absolute value of the vertical errors can not be derived due to the special geometry (Chen and Stewart, 2006). Furthermore, the worst situation is that before using hodograms to determine the back-azimuth of an event, the orientations of the downhole geophones have to be determined by using the direct or refracted wave generated by artificial shots, which unavoidably distorts the location. Press et al., (1999) developed a bootstrap method using a numerical technique for an ad-hoc error estimation, where the inversion procedure is repeated many times with random noise superposed on the synthetic data. Using his

method, Oye et al. (2003) finished a simulation of this by using a six-station VSP array to illustrate the error distributions. As a result, maximum extension is about  $\pm 50\text{m}$  for grid points 400m closer to the geophone tool.

Hence, compared with these conventional methods, hypocenter location using arrival times alone is a much more accurate, reliable and convenient method.

### CONCLUSIONS

We calculated the error distributions located by using the network composed of one to three VSP arrays and geophones in the surrounding wells. Rather than using the conventional location methods for the events recorded by a downhole VSP array, the calculation of the location accuracy based on P and/or S arrival times alone is much superior. Results indicate that the one-standard horizontal and vertical errors using the latter can be greatly reduced to 5m-10m within the network, which is much better than the former case.

We also found some rules of network arrangements, which can guide the future network design using the suggested arrival time method as follows.

- 1) Within the depth range of an existing array, the effect of the depth of newly-added geophones in separate wells seems insignificant to the depth.
- 2) The larger the scale of a network, the smaller the horizontal errors will be; vertical errors are insensitive to the scale of the network.
- 3) A network composed of three VSP arrays improves the accuracy of both horizontal and vertical location errors to 5m-10m within the space between them.
- 4) A network composed of a VSP and geophones in the surrounding multiple wells can reduce location errors to 5m-10m in the vicinity of the VSP.

### ACKNOWLEDGEMENTS

We thank the industrial sponsors of *CREWES* for their funding assistance.

### REFERENCES

- Chen Z.L. and Stewart R.R., 2006, Estimates of hypocenter location errors of passive microseismic events located by using a 3-C VSP array: *Ann. Internat. Mtg. Soc. Expl. Geophys.*, **25**, 1575-1579.
- Chen Z.L., 2006, Guidelines for the geometry design of local microseismic arrays: *CREWES Research report*, **18**.
- Evernden J.F., 1969, Precision of epicenters obtained by small numbers of world-wide stations: *Bulletin of the Seismological Society of America*, **59**, No.3, 1365-1398.
- Fabriol H., 2001, Saline aquifer CO<sub>2</sub> storage (SACS) feasibility study of microseismic monitoring (Task 5.8): Report of BRGM/RP-51293-FR.
- Flinn, E.A., 1965, Confidence regions and error determinations for seismic event location: *Rev. Geophys.* **3**, No.1, 157-185.

- Phillips W.S., Rutledge J.T. and Fairbanks T.D., 1998, Reservoir Fracture Mapping Using Microearthquakes: Two Oilfield Case Studies: Soc. Petrol. Eng. (SPE#36651), 11p.
- Oye, V. and Roth, M., 2003, Automated seismic event location for hydrocarbon reservoirs: Computers & Geosciences **29**, 851-863.
- Phillips, W.S. et al., 2000, Induced microearthquake patterns in hydrocarbon and geothermal reservoirs: report of Seismic Research Center, Los Alamos National Laboratory.
- Poupinet G., Ellsworth W.H. and Frechet J., 1984, Monitoring velocity variations in the crust using earthquakes doublets: An application to the Calaveras Fault, California: J.G.Res., **89**, 5719-5731.
- Rutledge et al., 1998, Reservoir characterization using oil-production-induced microseismicity, Clinton County, Kentucky: Tectonophysics, **289**, 129-152.